

The shape of pulsar radio beams

J. L. Han^{1,2}, R. N. Manchester³

¹*Beijing Astronomical Observatory of National Astronomical Observatories, CAS, Beijing 100012, China; hjl@bao.ac.cn*

²*Beijing Astrophysical Center, CAS-PKU, Beijing 100871, China*

³*Australia Telescope National Facility, CSIRO, PO Box 76, Epping, NSW 2121, Australia; rmanches@atnf.csiro.au*

Accepted ; Received ; in original form

ABSTRACT

Using all available multi-component radio pulse profiles for pulsars with medium to long periods and good polarisation data, we have constructed a two-dimensional image of the mean radio beamshape. This shows a peak near the centre of the beam but is otherwise relatively uniform with only mild enhancements in a few regions. This result supports the patchy-beam model for emission beams in which the mean beam shape represents the properties of the emission mechanism and observed pulse components result from emission sources distributed randomly across the beam.

Key words: Pulsars: general

1 INTRODUCTION

Pulsars are generally believed to be rotating neutron stars in which the observed pulses result from one or more emission beams sweeping across the Earth as the star rotates. Observations of radio polarisation (Radhakrishnan & Cooke 1969) led to the magnetic-pole model in which the emission beam was centred on the magnetic axis of a predominantly dipole magnetic field. On the assumption that the emission is directed radially, the observed pulse profile reflects the variations in emission intensity along a line of constant rotational latitude. Although more than 1000 pulsars are now known (Taylor, Manchester & Lyne 1993; Lyne et al. 2000) the shape of pulsar radio beams remains controversial.

There are two main areas of uncertainty. One concerns the outline shape of the radio beam. Originally assumed to be circular, some investigations (e.g. Narayan & Vivekanand 1983) argued for an elliptical beam extend in the latitude direction with a large axial ratio. In contrast, Biggs (1990) suggested that the beam was slightly compressed in the latitudinal direction. Most other investigations (e.g. Lyne & Manchester 1988; Björnsson 1998; Gil & Han 1996) have concluded that the emission beam is essentially circular, and we will assume this in the present investigation.

The second area of uncertainty concerns the form of the beam pattern. Early observations showed that there are two or more pulse components in many pulsars (e.g. Lyne, Smith & Graham 1971; Manchester 1971). Ruderman & Sutherland (1975) presented a detailed model for pulsar radio emission in which the beam had the shape of a hollow cone, more intense around the periphery, corresponding to the last open field lines emanating from the polar cap region. The radio emission was attributed to curvature radiation by positrons moving these field lines. Such radiation is linearly polarised

in the plane of curvature of the magnetic field and hence the model naturally explained the smooth sweep of polarisation position angle seen in many pulsars, as well as the common occurrence of double-peaked pulse profiles.

Backer (1976) first discussed the more-or-less central pulse component seen in many pulsars and suggested that it resulted from an axial beam. Rankin (1983) made the distinction between this central or ‘core’ emission and the outer or ‘conal’ emission, and showed that these two components of the profile had rather different properties. At least in short-period pulsars, core emission has a steeper spectrum than conal emission (Rankin 1983; Lyne & Manchester 1988) and the fluctuation properties of the two types of emission are very different (Rankin 1986). This model was subsequently extended to have two or more coaxial conal emission zones, either to account for multiple-component profiles (Gil & Krawczyk 1997; Qiao & Lin 1998) or for the appearance of components at different apparent radii from the conal axis (Rankin 1993a; Kramer et al. 1994; Mitra & Deshpande 1999). These latter analyses depend on a knowledge of the angle between the beam and rotation axes (α), usually computed from the observed width of a ‘core’ component. Unfortunately, the determination of this angle is very model dependent and this results in large uncertainties in the derived radii.

Based on a large sample of pulse shape and polarisation data, Lyne & Manchester (1988) found that pulse components in multiple-component profiles were not symmetrically located within the beam boundary. Furthermore, they were generally of very different intensities and, in some cases, missing altogether. Their results were consistent with components being randomly located within the beam boundary, leading to the ‘patchy-beam’ model. Gould (1994) and

arXiv:astro-ph/0010538v1 26 Oct 2000

Table 1. Normalized impact angles and the frequency of profile samples

PSR J	freq	β_n	PSR J	freq	β_n	PSR J	freq	β_n	PSR J	freq	β_n
J0102+6537	1408	0.27	J1136+1551	1408	0.69	J1807-0847	1408	0.25	J1954+2923	1408	0.70
J0108+6905	610	0.20	J1239+2453	1400	0.04	J1810-5338	660	0.93	J2002+4050	1408	0.55
J0152-1637	610	0.20	J1509+5531	925	0.52	J1816-2649	606	0.59	J2004+3137	1408	0.05
J0332+5434	925	0.26	J1559-4438	1502	0.39	J1823+0550	610	0.20	J2006-0807	1408	0.43
J0406+6138	610	0.21	J1604-4909	658	0.02	J1826-1334	1408	0.12	J2022+2854	925	0.52
J0450-1248	610	0.86	J1646-6831	660	0.02	J1829-1751	925	0.02	J2037+3621	606	0.36
J0452-1759	1404	0.58	J1651-1709	606	0.70	J1834-0426	606	0.30	J2046+1540	1408	0.53
J0528+2200	925	0.14	J1651-5222	658	0.54	J1841+0912	1408	0.31	J2048-1616	925	0.21
J0536-7543	663	0.26	J1703-3241	610	0.26	J1842-0359	1408	0.17	J2053-7200	658	0.18
J0624-0424	1408	0.21	J1720-2933	1408	0.68	J1847-0402	1408	0.35	J2055+2209	606	0.71
J0653+8051	1408	0.21	J1733-2228	610	0.69	J1848-0123	1642	0.40	J2113+4644	925	0.13
J0729-1836	610	0.67	J1735-0724	1408	0.02	J1900-2600	610	0.22	J2157+4017	610	0.45
J0754+3231	610	0.18	J1740+1311	1408	0.27	J1906+0641	1408	0.44	J2212+2933	610	0.26
J0837+0610	1408	0.74	J1741-0840	610	0.39	J1907+4002	1408	0.26	J2229+6205	610	0.41
J0846-3533	1440	0.07	J1745-3040	1642	0.03	J1912+2104	610	0.20	J2308+5547	1408	0.23
J0907-5157	660	0.52	J1748-1300	610	0.28	J1916+0951	610	0.68	J2317+2149	1408	0.38
J0908-1739	1408	0.57	J1750-3157	1408	0.21	J1919+0021	610	0.48	J2321+6024	925	0.59
J0921+6254	606	0.33	J1754+5201	1408	0.38	J1921+1948	610	0.57	J2324-6054	660	0.40
J0955-5304	658	0.02	J1756-2435	1408	0.31	J1921+2153	925	0.64	J2325+6316	610	0.13
J1034-3224	661	0.03	J1757-2421	1408	0.06	J1932+1059	1642	0.92	J2330-2005	1408	0.22
J1036-4926	658	0.34	J1801-2920	1440	0.02	J1945-0040	610	0.31	J2337+6151	1408	0.42
J1041-1942	925	0.34	J1803-2137	1408	0.27	J1948+3540	1408	0.36			

Gould, Lyne & Smith (2000) confirmed these conclusions with an even larger data set.

Manchester (1995) suggested an interpretation of these results in which the observed pulse profile is the product of a ‘window function’, which is a function of pulse period and radio frequency but common to all pulsars, and a ‘source function’ which determines the strength of the emission at a given point within the beam and is different for every pulsar. For example, the source function may be determined by the density or energy of the plasma beams along different field lines, whereas the window function is determined by the properties of the emission mechanism.

In this paper, we determine the two-dimensional shape of the window function at frequencies around 1 GHz by averaging the observed pulse profiles of multi-component pulsars having reliable polarisation data. This analysis depends only on the observed width of the pulse profile and the ‘impact parameter’, that is the minimum angle between the line of sight and the beam axis, usually given the symbol β . In contrast to the beam inclination angle α , the impact parameter is normally well determined from the maximum rate of change of position angle at the profile centre (Lyne & Manchester 1988). We assume that emission is seen across the entire polar cap and choose only pulsars with profiles where this appears to be the case. In Section 2 we describe the data set and our methods of determining the two-dimensional beam pattern. Results are presented and discussed in Section 3 and Section 4 summarises our conclusions.

2 THE DATA SET AND ANALYSIS METHOD

In order to reliably determine the two-dimensional beam shape we choose pulsars which have pulse profiles with two

or more pulse components, good signal/noise ratio and good quality polarisation data.

For most pulsars with two or more pulse components, we see emission from right across the polar cap. The polarisation information allows a measurement of the normalised impact angle, β_n , that is, the impact parameter β expressed as a fraction of the beam radius. This parameter is computed assuming $\alpha = 90^\circ$, but it is not very sensitive to the actual value of α (Lyne & Manchester 1988). The polarisation data also allow a check on the assumption that we are seeing emission right to both edges of the beam. Only those pulsars for which the maximum rate of change of position angle is close to the pulse centre were included in the sample. Single component pulsars are not included in the sample as it is often difficult to reliably determine if they are predominantly core emission (low β_n) or from the outer edge of the beam (high β_n).

Millisecond pulsars were also excluded from the sample as they generally have very wide and complex profiles and polarisation variations which do not fit the simple rotating-vector model (e.g. Navarro et al. 1997, Stairs et al. 1999). It is therefore difficult or impossible to obtain reliable values of β_n for these pulsars. Very short-period pulsars also commonly have wide or interpulse profiles and are excluded from the sample for similar reasons.

Pulse profiles in a given pulsar usually evolve with frequency, with some components becoming stronger and other becoming weaker or even disappearing at higher or lower frequencies. At low frequencies, the core component tends to dominate the profile, whereas at high frequencies the conal emission is generally dominant. To ensure relative uniformity in the data set, we restricted our attention to profiles at frequencies between 600 and 1600 MHz. The results we obtain therefore represent pulsar emission at frequencies around 1 GHz.

We checked the profiles available on the pulsar profile

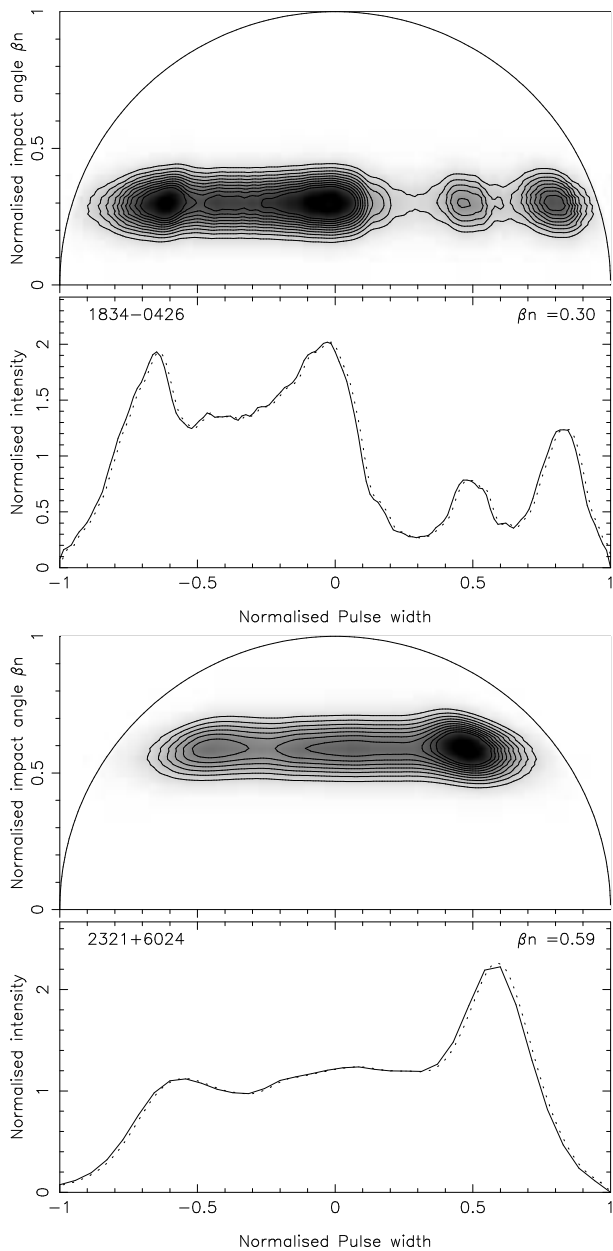


Figure 1. Beam components for four pulsars derived using the procedures described in Section 2. The pulse profiles are given in the lower panels where the dotted lines represent the interpolated profile used in the projection on to the beam pattern.

database^{*} of European Pulsar Network maintained at Max-Planck-Institut für Radioastronomie (Lorimer et al. 1998), which contains pulsar profiles from more than 50 papers, including the large datasets from Gould & Lyne (1998), Manchester, Han & Qiao (1998) and Hoensbroech & Xilouris (1997). Normalised impact parameters were obtained from Lyne & Manchester (1988), Rankin (1993), Gould (1994) and Manchester et al. (1998). The final data set of 87 pulsars which satisfy the above criteria is listed in Table 1.

To determine the average beamshape, we first defined the duration of each pulse profile by taking the points at

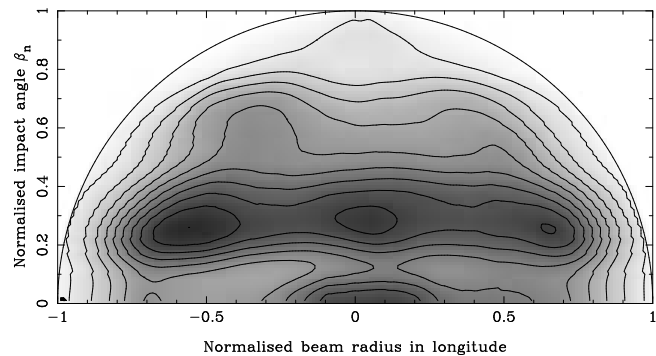


Figure 2. The beam pattern obtained by adding data for all pulsars in the sample represented as a greyscale. This pattern has not been normalised for the nonuniform distribution of β_n .

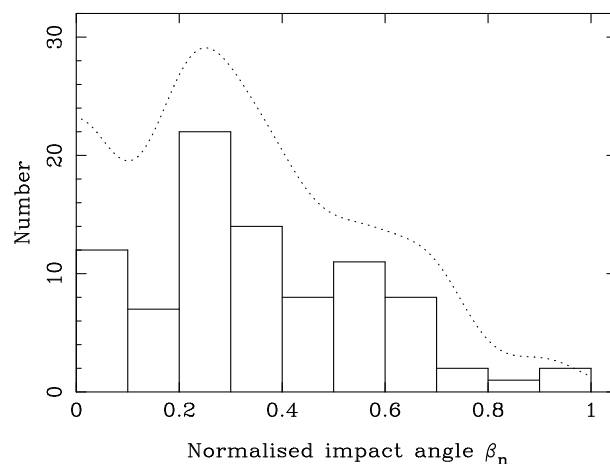


Figure 3. Distribution of normalised impact parameters, β_n , for pulsars in the sample. The dotted line is the sum of the gaussian-broadened values used in the projection (see text).

which the signal rose above 3σ , where σ is the rms deviation of the off-pulse noise. Next, the mean intensity of the observed emission within the pulse was normalised to unity. The normalised impact parameter, β_n , gives the offset of the locus of line of sight across the polar cap in the latitude direction as a fraction of the beam radius. We assumed a circular beam of unity radius and a straight trajectory of the emission point across the polar cap. The beamshape is assumed to be symmetric about the equator, i.e., the sign of β_n is ignored.

The profile intensity was interpolated on to an $x-y$ array representing a semi-circular beam of unity radius along a line at $y = \beta_n$ between x values of $\pm\sqrt{1 - \beta_n^2}$ using a five-point polynomial interpolation routine (Press et al. 1992). To allow for uncertainties in the value of β_n , possible nonlinearities in the beam trajectory across the polar cap, and to represent the finite width of a subpulse beam, the pulse profile is broadened in latitude (y) assuming a gaussian form, $\exp[-(\beta - \beta_n)^2/0.1]$, between $\Delta\beta = \pm 0.3$. Examples of computed beam components for two pulsars are shown in Fig. 1.

^{*} See <http://www.mpifr-bonn.mpg.de/div/pulsar/data/>

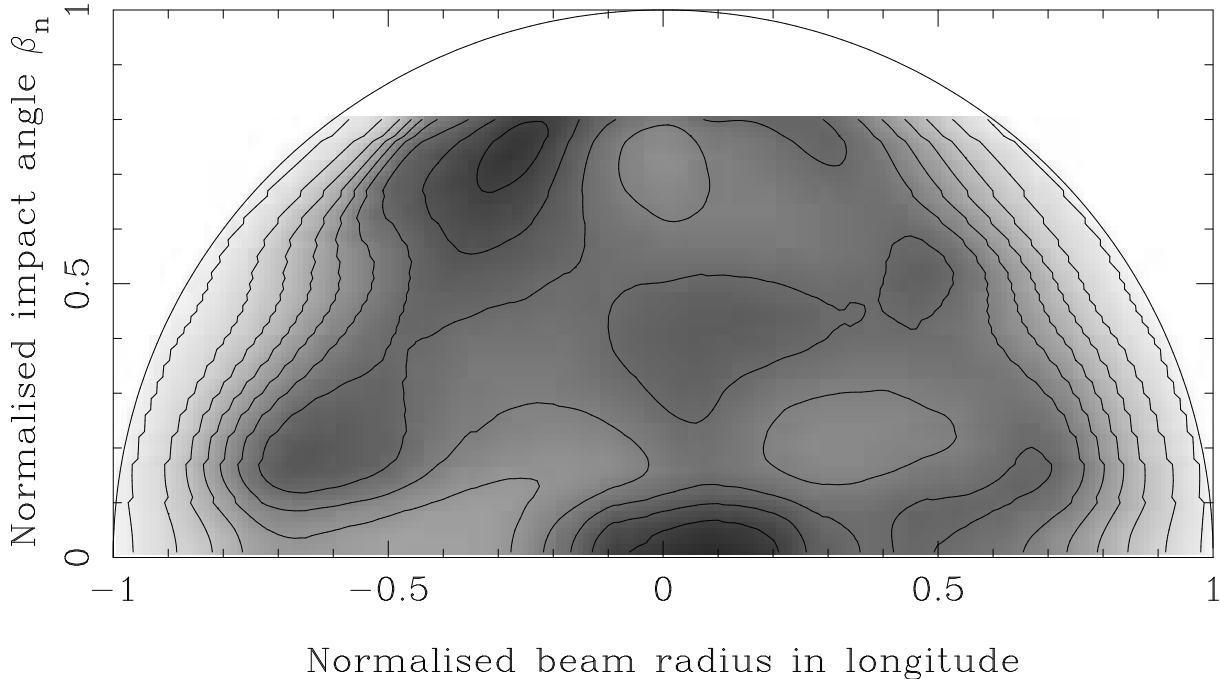


Figure 4. Average shape of the pulsar radio beam for $\beta_n < 0.8$. The contours are at multiples of 0.1 of the peak value near the beam center.

3 RESULTS AND DISCUSSION

Integrating all pulse profiles in the sample gives the beam shape shown in Fig. 2. This figure represents the probability of observing beam components at each location. However, it is strongly affected by the sample distribution of β_n . As shown in Fig. 3, this has a strong peak at $\beta_n \sim 0.25$, indicating that multi-component pulse profiles are most likely to be detected at about this impact parameter. The deficit at $\beta_n \sim 0$ is an observational selection effect which results from the smearing of rapid position angle changes near the profile centre due to finite subpulse beamwidths and instrumental broadening of the profile. Few multi-component profiles are observed at high β_n .

The beam distribution shown in Fig. 2 was normalised to correct for the non-uniform distribution of β_n using the gaussian-smoothed distribution shown in Fig. 3, giving the final average beam shape shown in Fig. 4. Since there are only one or two pulsars in bins with $\beta_n > 0.8$ (Fig. 3), there is large statistical uncertainty in the average profile shape for these bins. Therefore we do not plot this region of the normalised beam pattern.

The overall impression given by Fig. 4 is that of a ‘patchy’ beam. There are some systematic features, but in general the intensity is relatively uniform across the whole beam. The central or ‘core’ feature is significantly displaced toward later longitudes. The next most prominent property of the average beam after the core component is the presence of a few patches of slightly enhanced emission. Most of these are located within an irregular and rather broad annular maximum at a normalised radius of about 0.7 which is somewhat stronger on the leading side of the beam. Underlying this is more-or-less uniform emission over the whole of the emission beam. The decline at the beam edge is not very sharp.

Although there is no evidence for double or multiple cones in Fig. 4, our present data set is dominated by two- and three-component pulsars. A larger sample of pulsars with more than three components is needed to reliably distinguish multiple-cone models from a patchy beam models. However, our results suggest that, if multiple cones exist, they are at different radii relative to the beam radius in different pulsars. They also show that the conal emission is not confined to a single annular region at the beam boundary.

These results are consistent with the idea that components in pulse profiles are largely determined by the distribution of sources across the polar cap – the ‘source function’. The rather smooth distribution of intensity in the mean beam shape suggests that these source regions are randomly distributed for different pulsars as suggested by Lyne & Manchester (1988) and Manchester (1995) – the ‘patchy-beam’ model. The number of identifiable source components across the profile is mostly limited by the finite width of subpulse beams. Except in a few cases with very high signal/noise ratio, e.g. PSR B0740–28 (Kramer 1994), it is generally not possible to identify more than four or five peaks or components, and often only one or two. Some very wide components identified by gaussian fitting, e.g. PSRs B2319+60, B2021+51 (Kramer 1994), are most probably regions of distributed emission producing overlapping subpulse beams.

We believe Fig. 4 is a good representation of the *mean* radio beam (for $\beta_n < 0.8$) emitted at frequencies around 1 GHz by ‘typical’ pulsars, that is, the pulsars of medium or long period which dominate the sample of known radio pulsars. It represents the ‘window function’ in the model of Manchester (1995) which is determined by the effective gain or efficiency of the radio emission process.

4 CONCLUSIONS

We have computed the average radio beamshape at frequencies about 1 GHz of pulsars with medium to long periods. This beamshape has a peak near its centre and a mild, broad and rather irregular enhancement at a normalised beam radius of about 0.7, but is otherwise rather uniform. The decline at the beam edge is gradual.

These results suggest that the presence and location of profile components are determined by a ‘source function’ which varies randomly from pulsar to pulsar. The summing of these randomly distributed components results in a relatively uniform average beam profile which we interpret as the ‘window function’ representing the properties of the emission process common to all longer-period pulsars.

ACKNOWLEDGMENTS

We thank Prof. Qiao Guojun and Zhao Yongheng for helpful discussions and the referee for helpful comments. This work was initiated during JLH’s visit to the ATNF during 1997. JLH thanks the Su Shu Huang Astrophysics Research Foundation of CAS and the exchange program between CAS and CSIRO for support of visits in 1997 and 1999, respectively. His work in China is supported by the National Natural Science Foundation of China and the National Key Basic Research Science Foundation. The profile data were obtained from the pulsar database of the European Pulsar Network at the Max-Planck-Institut für Radioastronomie. The Australia Telescope is funded by the Commonwealth Government for operation as a National Facility managed by CSIRO.

REFERENCES

- Backer D. C., 1976, *ApJ*, 209, 895
 Biggs J. D., 1990, *MNRAS*, 245, 514
 Björnsson C I., 1998, *AA*, 338, 971
 Gil J. A., Han J. L., 1996, *ApJ*, 458, 265
 Gil J., Krawczyk A., 1997, *MNRAS*, 285, 561
 Gould D. M., Lyne A. G., 1998, *MNRAS*, 301, 235
 Gould D. M., 1994, PhD thesis, The University of Manchester
 Gould D. M., Lyne A. G., Smith F. G., 2000, *MNRAS*, Submitted
 Hoensbroech A. v., Xilouris K. M., 1997, *A&AS*, 126, 121
 Kramer M., 1994, *A&AS*, 107, 527
 Kramer M., Wielebinski R., Jessner A., Gil J. A., Seiradakis J. H., 1994, *A&AS*, 107, 515
 Lorimer D. R., Jessner A., Seiradakis J. H., Lyne A. G., D’Amico N., Athanasopoulos A., Xilouris K. M., Kramer M., Wielebinski R., 1998, *A&AS*, 128, 541
 Lyne A. G., Manchester R. N., 1988, *MNRAS*, 234, 477
 Lyne A. G. et al., 2000, *MNRAS*, 312, 698
 Lyne A. G., Smith F. G., Graham D. A., 1971, *MNRAS*, 153, 337
 Manchester R. N., 1971, *ApJS*, 23, 283
 Manchester R. N., 1995, *JA&A*, 16, 107
 Manchester R. N., Han J. L., Qiao G. J., 1998, *MNRAS*, 295, 280
 Mitra D., Deshpande A. A., 1999, *A&A*, 346, 906
 Narayan R., Vivekanand M., 1983, *A&A*, 122, 45
 Navarro J., Manchester R. N., Sandhu J. S., Kulkarni S. R., Bailes M., 1997, *ApJ*, 486, 1019
 Press W. H., Teukolsky S. A., Vetterling W. T., Flannery B. P., 1992, *Numerical Recipes: The Art of Scientific Computing*, 2nd edition. Cambridge University Press, Cambridge

- Qiao G. J., Lin W. P., 1998, *A&A*, 333, 172
 Radhakrishnan V., Cooke D. J., 1969, *Astrophys. Lett.*, 3, 225
 Rankin J. M., 1983, *ApJ*, 274, 359
 Rankin J. M., 1986, *ApJ*, 301, 901
 Rankin J. M., 1993a, *ApJ*, 405, 285
 Rankin J. M., 1993b, *ApJS*, 85, 145
 Ruderman M. A., Sutherland P. G., 1975, *ApJ*, 196, 51
 Stairs I. H., Thorsett S. E., Camilo F., 1999, *ApJS*, 123
 Taylor J. H., Manchester R. N., Lyne A. G., 1993, *ApJS*, 88, 529